

## DETECTION OF AN IRON EMISSION FEATURE FROM THE LENSED BAL QSO H1413+117 AT $Z = 2.56$

T. OSHIMA<sup>1,2</sup>, K. MITSUDA<sup>1</sup>, R. FUJIMOTO<sup>1</sup>, N. IYOMOTO<sup>1</sup>, K. FUTAMOTO<sup>1</sup>, M. HATTORI<sup>3</sup>,  
 N. OTA<sup>1,4</sup>, K. MORI<sup>5</sup>, Y. IKEBE<sup>6</sup>, J.M. MIRALLES<sup>3,7,8</sup>, AND J-P. KNEIB<sup>9</sup>

*Submitted to ApJ Letters on July 4 , 2001*

### ABSTRACT

We present the X-ray energy spectrum of the lensed BAL QSO H1413+117 (the Cloverleaf) at  $z = 2.56$  observed with the *Chandra* X-ray observatory. We detected 293 photons in a 40 ks Advanced CCD Imaging Spectrometer (ACIS-S) observation. The X-ray image consists of four lensed image components, thus the photons are from the lensed QSO itself. The overall spectrum can be described with a power-law function heavily absorbed by neutral matter at a redshift consistent with the QSO redshift. This supports the idea that intrinsic absorption is significant for BAL QSOs. The spectral fit significantly (99 % confidence) improves when we include an emission line. The centroid energy and intrinsic width (Gaussian  $\sigma$ ) of the line are  $6.21 \pm 0.16$  keV and  $220_{-130}^{+270}$  eV (90 % errors), respectively, in the QSO rest frame, assuming the absorbed power-law as the continuum. The equivalent width of the line in the QSO rest frame is  $960_{-480}^{+1400}$  eV. We suggest that the large equivalent width, the centroid energy, and the line broadness can be explained by iron K emission arising from X-ray reprocessing in the BAL flow, assuming it has a conical thin-sheet structure.

*Subject headings:* quasars: emission lines — quasars: individual (H1413+117) — gravitational lensing — X-rays: galaxies

### 1. INTRODUCTION

H1413+117 (the Cloverleaf) is a QSO at a redshift of  $z=2.56$ , gravitationally lensed into four image components with an angular separation of  $\sim 1''$  (Magain et al. 1988); though the exact nature of the lens object(s) remains elusive (Kneib et al. 1998; Kneib, Alloin, & Pello 1998). The optical spectrum of the QSO shows broad absorption features, hence it is classified as a broad absorption line (BAL) QSO (Hazard et al. 1984).

BAL QSOs are in general extremely faint in X-rays (Green et al. 1995; Green & Mathur 1996, hereafter G1995; GM1996). ROSAT, ASCA, and recent *Chandra* studies have shown that BAL QSOs are X-ray faint because of a large intrinsic absorption ( $N_{\text{H}} > 10^{23} \text{ cm}^{-2}$ ) and that the QSO itself is as bright as typical radio quiet QSOs (Gallagher et al. 1999; Brinkmann et al. 1999; Green et al. 2001, hereafter G2001). Wang et al. (2000) examined the ionization state of the X-ray absorber and concluded that the absorbers for the UV broad absorption lines and X-ray absorption can be the same, although partial covering needs to be assumed for some of the UV absorbers. Elvis (2000) proposed an empirical model in which narrow absorption line QSOs, BAL QSOs, and ordinary QSOs are unified.

X-ray emission from H1413+117 was detected at the 3

$\sigma$  level with a 28 ks ROSAT PSPC observation (Chartas 2000). We observed H1413+117 with the *Chandra* Advanced CCD Imaging Spectrometer (ACIS-S) for 40 ks. The high sensitivity of *Chandra* and the magnification of the gravitational lens enabled the detection of a strong emission line from this distant BAL QSO. In this letter we report on the X-ray energy spectrum and discuss the implications for BAL QSO X-ray emission : analysis of the X-ray image will be published in a separate paper.

### 2. OBSERVATION AND RESULTS

We observed H1413+117 on 2000 April 19 with the *Chandra* observatory. The data were obtained using the back-illuminated ACIS-S3 chip at a CCD temperature of  $-120^{\circ}\text{C}$ , and processed using CIAO 2.1 with CALDB 2.6. After the standard data screening, the net observation time was 38.2 ks. The data contained a few background flares with about 2 times the nominal background rate. Since the contamination from the background flares in the point source is small, we did not filter these periods, however, we eliminated all the flares when making the background spectrum. A total of 293 X-ray events had spatial positions consistent with H1413+117 within the systematic errors of *Chandra*'s attitude solution ( $\sim 2''^{10}$ ). The X-ray emission is spatially extended compared to the point spread function of the X-ray mirror. The extension is con-

<sup>1</sup> Institute of Space and Astronautical Science, Sagamihara, Kanagawa, 229-8510, Japan

<sup>2</sup> oshima@astro.isas.ac.jp

<sup>3</sup> Astronomical Institute, Tōhoku University, Sendai, 980-8578, Japan

<sup>4</sup> Department of Physics, Tokyo Metropolitan University, Hachioji, Tokyo, 192-0397, Japan

<sup>5</sup> Department of Earth and Space Science, Graduate School of Science, Osaka University, Toyonaka, Osaka, 560-0043, Japan

<sup>6</sup> Max-Planck-Institut für Extraterrestrische Physik, Postfach 1312, D-85741, Garching, Germany

<sup>7</sup> ST-ECF, Karl-Schwarzschild Str. 2, Garching bei München D-85748, Germany

<sup>8</sup> IAEF der Universität Bonn, Auf Dem Hügel 71, D-53121 Bonn, Germany

<sup>9</sup> Observatoire Midi-Pyrénées, UMR 5572, 14 Avenue E.Belin, F-31400 Toulouse, France

<sup>10</sup> <http://asc.harvard.edu/mta/ASPECT/celmon/index.htm>

sistent with the sum of the four gravitationally lensed images of the QSO. The image (Figure 1), reconstructed using the method proposed by Tsunemi et al. (2001) and revised for faint sources by Mori et al. (2001), in which subpixel spatial resolutions can be obtained for charge-split events, shows that X-ray photons come from positions consistent with those of the four lensed images. However, the intensity ratios of the four images are not consistent with those at optical wavelengths within the statistical errors; image A is relatively brighter in X-rays than in the optical. Further details of the image analysis and their implications will be published in a separate paper.

We then constructed an X-ray energy spectrum and performed model fits. We created the telescope/detector response functions according to the standard procedure provided by the *Chandra* science center. The subtracted background spectrum was estimated from an annular region with an outer radius of  $130''$  and an inner radius of  $4''$ . We confirmed that there is no significant position dependency of the background counting rate by changing the outer radius of the background region from  $30''$  to  $130''$ . The background counting rate is only 1% of the source counting rate, and is negligible compared to the statistical errors of the source spectrum. Before performing the model fit, we binned the spectrum to a minimum of 20 photons per energy bin.

We first fitted the spectrum with a power-law function absorbed by neutral matter. We included two absorption components assuming the solar abundance (Anders & Grevesse 1989); the absorption in our Galaxy with a hydrogen column density  $N_{\text{H}}$  fixed to  $1.78 \times 10^{20} \text{ cm}^{-2}$  (Stark et al. 1992), and the absorption at a redshift of  $z_{\text{abs}}$ . With  $z_{\text{abs}}$  set free, it converged to  $z_{\text{abs}} = 2.55^{+0.27}_{-0.18}$  with  $N_{\text{H}} = 2.4^{+1.5}_{-1.2} \times 10^{23} \text{ cm}^{-2}$  (90 % errors, see Table 1) and  $\chi^2 = 12.8$  for 10 degrees of freedom (dof), well constrained by its iron K-edge. However since the edge energy in the observer frame (2.00 keV) is close to that of the Iridium M-V edge (2.04 keV) of the mirror response function, we need to be careful about the calibration. We thus derived the energy spectra of some QSOs in the archival data observed within 2 months of our observation. We found that the spectra does not require any additional absorption structure even if we vary the edge energy around the Iridium edge. We obtained  $N_{\text{H}} < 1 \times 10^{22} \text{ cm}^{-2}$  as the 90 % upper limit of the absorption at  $z_{\text{abs}} = 2.56$  in the archival data, which is an order of magnitude smaller than that we obtained for H1413+117. Thus the absorber is likely to be at the redshift of H1413+117 and we fix  $z_{\text{abs}}$  at 2.56 from now on.

Although the fit is acceptable at the 91 % confidence level, the residual of the fit shows  $2\sigma$  excesses in adjacent bins around 1.7 keV ( $\sim 6.2$  keV in the QSO rest frame). We therefore masked out these bins and those either side (Figure 2(a)), and fitted an absorbed power-law function. The  $\chi^2$  value became significantly smaller ( $\chi^2 = 2.7$  for 7 dof). The assumption that the residuals of those two energy bins obey the same statistics as other energy bins is rejected by an  $F$ -test at the 99 % confidence level. In Figure 2(a) we show the residuals of data against this model, which indicates an emission line. We thus tried including an additional spectral component to describe the

excess emission; a Gaussian line feature and a power-law component of different absorption column density. In the latter model, we linked the power-law index  $\Gamma$  of the second power-law component with the first one, similar to the partial absorption model proposed by (G2001) if the absorption column density of the second power-law component is small. The best-fit  $\chi^2$  value was 10.9 for 9 dof for the latter model giving the improvement only at the 60 % level significance. On the contrary, the resultant  $\chi^2$  value of the Gaussian model was 2.8 for 8 dof and the improvement of the fit from the model without a line was again 99 % with an  $F$ -test.

In Table 1, we show the best-fit spectral parameters. The intrinsic absorption is again strong ( $N_{\text{H}} = 1.9^{+1.0}_{-0.8} \times 10^{23} \text{ cm}^{-2}$ ). The centroid energy  $E_c$  of the line is  $6.21 \pm 0.16$  keV in the QSO rest frame. Thus the neutral iron K emission line at 6.4 keV is just outside the error domain. An intrinsically narrow emission line is also outside the 90 % statistical errors (Gaussian  $\sigma = 220^{+270}_{-130} \text{ eV}$ ). The equivalent width (EW) is  $270^{+390}_{-130} \text{ eV}$  ( $960^{+1400}_{-480} \text{ eV}$  in the QSO rest frame). We also performed a fit forcing the line to be intrinsically narrow: in this case, the improvement of the fit from a power-law is still significant at the 99% level. We obtained similar values for  $E_c$  and EW. We checked the calibrations of the energy scale and the energy resolution of the detector with archival data of SNRs and QSOs observed within 2 months of our observation. From the energy spectra accumulated within the same image region in the detector coordinates that we used for H1413+117, we found that the energy scale and the resolution are correct within 2 % ( $\sim 120$  eV) and 20 % ( $\sim 40$  eV in FWHM), respectively. The *Chandra* calibration web site <sup>11</sup> states that the uncertainty in the resolution is at most 40 %. Thus 6.4 keV can be inside the error domain if we consider the calibration uncertainty. However the line still needs to be broad assuming an absorbed power-law model as the continuum. The line parameters also depend on the choice of the continuum and because of the unusually small  $\Gamma = 1.33^{+0.25}_{-0.48}$  we tested whether the addition of a highly absorbed power-law, or a non-absorbed power-law component gave any improvement. The resultant fits for  $\Gamma$  are  $1.55 \pm 0.6$ ,  $1.34^{+0.7}_{-0.5}$  respectively, with larger statistical errors. Although the best-fit values of line parameters are not sensitive to these choices of continuum, we obtained larger statistical errors. As a result,  $E_c = 6.4$  keV and zero intrinsic width are included in the error domain.

From the best-fit spectral model function we estimated the slope  $\alpha_{\text{OX}}$  of a power-law connecting the rest frame  $2500 \text{ \AA}$  and 2 keV flux densities (neglecting possible differences in the X-ray and optical magnification factors) to be  $3.31 \pm 0.15$ . This is not only steeper than the average  $\alpha_{\text{OX}} = 1.57 \pm 0.15$  of normal QSOs (G1995) but also steeper than that of the *Chandra* BAL survey QSOs (G2001). Correcting for the intrinsic absorption we obtain  $\alpha_{\text{OX}} = 1.87 \pm 0.15$  which is consistent with normal QSOs, implying that BAL QSOs are obscured by strong absorption. Finally, the X-ray luminosity in the 0.5–6 keV band (1.8–21 keV in the QSO rest frame) is estimated to be  $3.4 \times 10^{45} \text{ erg/s}$  assuming  $H_0 = 50 \text{ km/s/Mpc}$  and  $q_0 = 0.5$ , where we corrected only for the galactic absorp-

<sup>11</sup> <http://asc.harvard.edu/ciao2.1/caveats/specres.html>

tion. The luminosity is  $5.0 \times 10^{45}$  erg/s if we also correct for the intrinsic absorption of the continuum. Since the magnification of the lens is estimated to be  $\sim 10$  (Chartas 2000), the true luminosity of the QSO is a factor of 10 lower than the above values.

### 3. DISCUSSION

The observed EW of the emission line,  $960^{+1400}_{-480}$  eV in the QSO rest frame, is an order of magnitude larger than those of typical Seyfert 1 galaxies (e.g. Mushotzky, Done, & Pounds 1993). The large EW suggests that a considerable part of direct beam of the ionizing X-rays is blocked by some intervening material, while the reprocessed emission is not significantly absorbed. Thus we need some low-ionization material which partly covers the central engine and serves as an efficient X-ray reprocessor. A candidate for such beam blockers and/or reprocessors is the BAL flow. The BAL flow is believed to be a mass flow with velocities of  $1 - 6 \times 10^4$  km/s along the line of sight. If the flow is neither aligned with the accretion-disk plane nor the disk axis, and if the system is axially symmetric, the flow must have a conical structure, as proposed by Elvis (2000). The BAL flow is believed to cover about 10–50 % of the solid angle around the central engine (Krolik & Voit 1998; Goodrich 1997). Then the BAL flow may be a conical thin sheet irradiated from the apex of the cone. According to Elvis (2000), the conical BAL flow is optically-thick in the direction of X-ray irradiation while it is optically thin in other directions for photons above  $\gtrsim 6$  keV (see Figure 3). Then almost all X-ray photons from the central source that enter the BAL flow are either absorbed or scattered, while the most of re-emitted and scattered photons escape from the flow (Elvis 2000). Thus in spite of the small covering solid angle, the conical BAL flow can be a more effective X-ray reprocessor than a molecular torus or an accretion disk, for which the reprocessing efficiency is limited by self-absorption. Although a conical BAL flow is not the only possibility, it is worth studying in more detail. Assuming the above geometry, the total intensities of the iron K emission and the Thomson scattered photons are estimated as,

$$F_{\text{FeK}} \sim \eta \frac{E_K F(E_K) \Omega_{\text{BAL}}}{\Gamma - 1} \frac{1}{4\pi} \omega_K f_{\text{FeK}}, \quad (1)$$

and

$$F_{\text{sca}}(E) \sim F(E) \frac{\sigma_{\text{sca}}}{\sigma_{\text{sca}} + \sigma_{\text{abs}}(E)} \frac{\Omega_{\text{BAL}}}{4\pi}, \quad (2)$$

where  $F(E)$  is the photon emission spectrum from the central X-ray source integrated over  $4\pi$  solid angle and is proportional to  $E^{-\Gamma}$ , and  $E_K$ ,  $\sigma_{\text{sca}}$ ,  $\sigma_{\text{abs}}(E)$ ,  $\Omega_{\text{BAL}}$ ,  $\omega_K$ , and  $f_{\text{FeK}}$  are respectively, the edge energy, the electron-scattering cross section, the absorption cross section, the solid angle of the BAL flow, the iron K fluorescence yield, and the fraction of iron K absorption over the entire absorption for the photons above the K edge energy. The factor,  $\eta$ , is defined as  $\eta = \int_{E_K}^{\infty} (\sigma_{\text{abs}}(E) / (\sigma_{\text{sca}} + \sigma_{\text{abs}}(E)) F(E) dE) / \int_{E_K}^{\infty} F(E) dE$ , and is 0.30 for  $\Gamma = 1.8$ , assuming the BAL flow to be neutral and of solar abundance.

The highest EW, expected when the direct X-ray photon beam from the central source is totally blocked, is

$$EW_{\text{max}} = \frac{F_{\text{FeK}}}{F_{\text{sca}}(E_e)} \sim 3.3 \text{ keV} \left( \frac{\eta}{0.3} \right) \left( \frac{f_{\text{FeK}}}{1} \right) \left( \frac{\omega_K}{0.35} \right), \quad (3)$$

where  $E_e$  is the line energy. On the other hand, when the central engine is directly visible, the EW is the lowest;

$$EW_{\text{min}} = \frac{F_{\text{FeK}}}{F(E_e)} \times \frac{1}{2} \sim 60 \text{ eV} \left( \frac{\eta}{0.3} \right) \left( \frac{\Omega_{\text{BAL}}/4\pi}{0.15} \right) \left( \frac{f_{\text{FeK}}}{1} \right) \left( \frac{\omega_K}{0.35} \right) \quad (4)$$

The factor 1/2 is included because one of the two BAL cones may be behind the accretion disk and not be visible to the observer. Thus the large observed EW can be explained if most of the direct beam is blocked by the BAL flow, which is generally believed to be the case for BAL QSOs. Then the observed continuum spectrum is dominated by the scattered photons as described by eq. 2. This spectrum is better approximated by a partial absorption model (G2001) than a single absorption model. However in the present observation, we do not have enough statistics to distinguish between these two.

Depending on the inclination angle to the line of sight and the cone angle of the BAL flow,  $\theta$ , the iron emission line originating from a certain portion of the BAL cone is either blue or red shifted. For BAL QSOs, our line of sight is aligned with the BAL flow of a certain azimuthal angle. Then most of iron emission we observe is from the far side of the cone, and is redshifted with energy shifts ranging from 0 to  $v_{\text{BAL}}/c \times |\cos(2\theta)|$  if  $\theta > 45$  deg. Thus the center of the emission line is redshifted and the line is broad. For H1413+117, the velocity of the BAL flow is  $\sim 0.04c = 12000$  km/s (Hazard et al. 1984) which implies a maximum energy shift of  $\sim 200$  eV if  $\theta \sim 70$  deg. Thus the energy shift and the broadness of the line suggested from the present observation are roughly consistent with these estimations.

Although the significance of the line itself is at the 99% confidence level, the line parameters are not well constrained because of the limited statistics, possible calibration uncertainties, and also possible uncertainties of the continuum spectrum. Since the centroid energy and the line broadening are key signatures of the reprocessing in the BAL flow, further observations with better statistics and/or better energy resolutions will be indispensable.

Finally we would like to point out that if the line of sight was inside the BAL cone, we should observe a blueshifted emission line, or both blueshifted and redshifted lines depending on the inclination angle. Since the direct beam would be visible in this case, the EW of the line would be  $\sim 60$  eV. These line features look similar to the broad line features observed in some Seyfert galaxies which are often described with disk-line models. Thus reprocessing in the BAL flow may at least partly account for those broad lines. Recently the detection of a redshifted broad strong (EW  $\sim 600$  eV) line feature in the X-ray spectrum of a Seyfert 2 galaxy at  $z \sim 1$  is reported (G. Hasinger 2001, private communication). We conjecture that this may have some connection to the emission line of H1413+117.

We thank P. Edwards for reviewing the manuscript. K.M. is grateful to W. Brinkmann for valuable discussions. N.O. and N.I. are supported by the JSPS Research Fellowship for Young Scientists. JPK acknowledges support from CNRS.

## REFERENCES

Anders, E., & Grevesse, N., 1989, *Geochim. Cosmochim. Acta*, 53, 197

Brinkmann, W., Wang, T., Matsuoka, M., & Yuan, W., 1999, *A&A*, 345, 43

Chae, K-H., & Turnshek, D.A., 1999, *ApJ*, 514, 587

Chartas, G., 2000, *ApJ*, 531, 81

Elvis, M., 2000, *ApJ*, 545, 63

Gallagher, S.C. et al., 1999, *ApJ*, 519, 549

Green, P.J. et al., 1995, *ApJ*, 450, 51

Green, P.J., & Mathur, S., 1996, *ApJ*, 462, 637

Green, P.J., Aldcroft, T.L., Mathur, S., Wilkes, B.J., & Elvis, M., 2001, *ApJ*, 558, 109

Goodrich, R.W., 1997, *ApJ*, 474, 606

Hazard, C., Morton, D.C., Terlevich, R., & McMahon, R., 1984, *ApJ*, 282, 33

Kneib, J-P., Alloin, D., Mellier, Y., Guilloteau, S., Barvainis, R., & Antonucci, R., 1998a, *A&A*, 329, 827

Kneib, J-P., Alloin, D., & Pello, R., 1998b, *A&A*, 339, L65

Krolik, J.H., & Voit, G.M., 1998, *ApJ*, 497, L5

Magain, P., Surdej, J., Swings, J.-P., Borgeest, U., Kayser, R., Kuehr, H., Refsdal, S., & Remy, M., 1988, *Nature*, 334, 325

Mori, K., Tsunemi, H., Miyata, E., Baluta, C., Burrows, D.N., Garmire, G.P., & Chartas, G., 2001, in *ASP Conf. Ser.* 251, *New Century of X-ray Astronomy*, ed. H. Inoue & H. Kunieda (San Francisco: ASP), 576

Mushotzky, R.F., Done, C., & Pounds, K.A., 1993, *ARA&A*, 31, 717

Stark, A.A., Gammie, C.F., Wilson, R.W., Bally, J., Linke, R.A., Heiles, C., & Hurwitz, M., 1992, *ApJS*, 79, 77

Tsunemi, H., Mori, K., Miyata, E., Baluta, C., Burrows, D.N., Garmire, G.P., & Chartas, G., 2001, *ApJ*, 554, 496

Wang, T.G., Brinkmann, W., Yuan, W., Wang, J.X., & Zhou, Y.Y., 2000, *ApJ*, 545, 77

TABLE 1  
RESULTS OF SPECTRAL FITS OF THE TOTAL SPECTRUM.

Parameter	Unit	Power-law	Power-law + line
$N$ <sup>a</sup>	$10^{-5}$ photon $\text{keV}^{-1} \text{cm}^{-2} \text{s}^{-1}$	$24_{-11}^{+25}$	$8.6_{-4.2}^{+6.8}$
$\Gamma$		$1.76 \pm 0.50$	$1.33_{-0.48}^{+0.25}$
$N_{\text{H}}$ <sup>b</sup>	$10^{23} \text{ cm}^{-2}$	$2.4_{-1.2}^{+1.5}$	$1.9_{-0.8}^{+1.0}$
$z_{\text{abs}}$		$2.55_{-0.18}^{+0.27}$	2.56 (fixed)
$E_e$ <sup>c</sup>	keV		$6.21 \pm 0.16$
$\Delta E (\sigma)$ <sup>c</sup>	eV		$220_{-130}^{+270}$
$EW$ <sup>c</sup>	eV		$960_{-480}^{+1400}$
reduced $\chi^2$		1.61	0.35
d.o.f.		10	8

<sup>a</sup>The normalization of power-law functions. X-ray flux at 1 keV in the QSO rest frame.

<sup>b</sup>The hydrogen column density at the redshift of  $z_{\text{abs}}$ .

<sup>c</sup>The values in the QSO rest frame.

Note. — Galactic absorption of a fixed column density of  $1.78 \times 10^{20} \text{ cm}^2$  is included in both models. The quoted errors correspond to a single parameter error at 90% confidence.

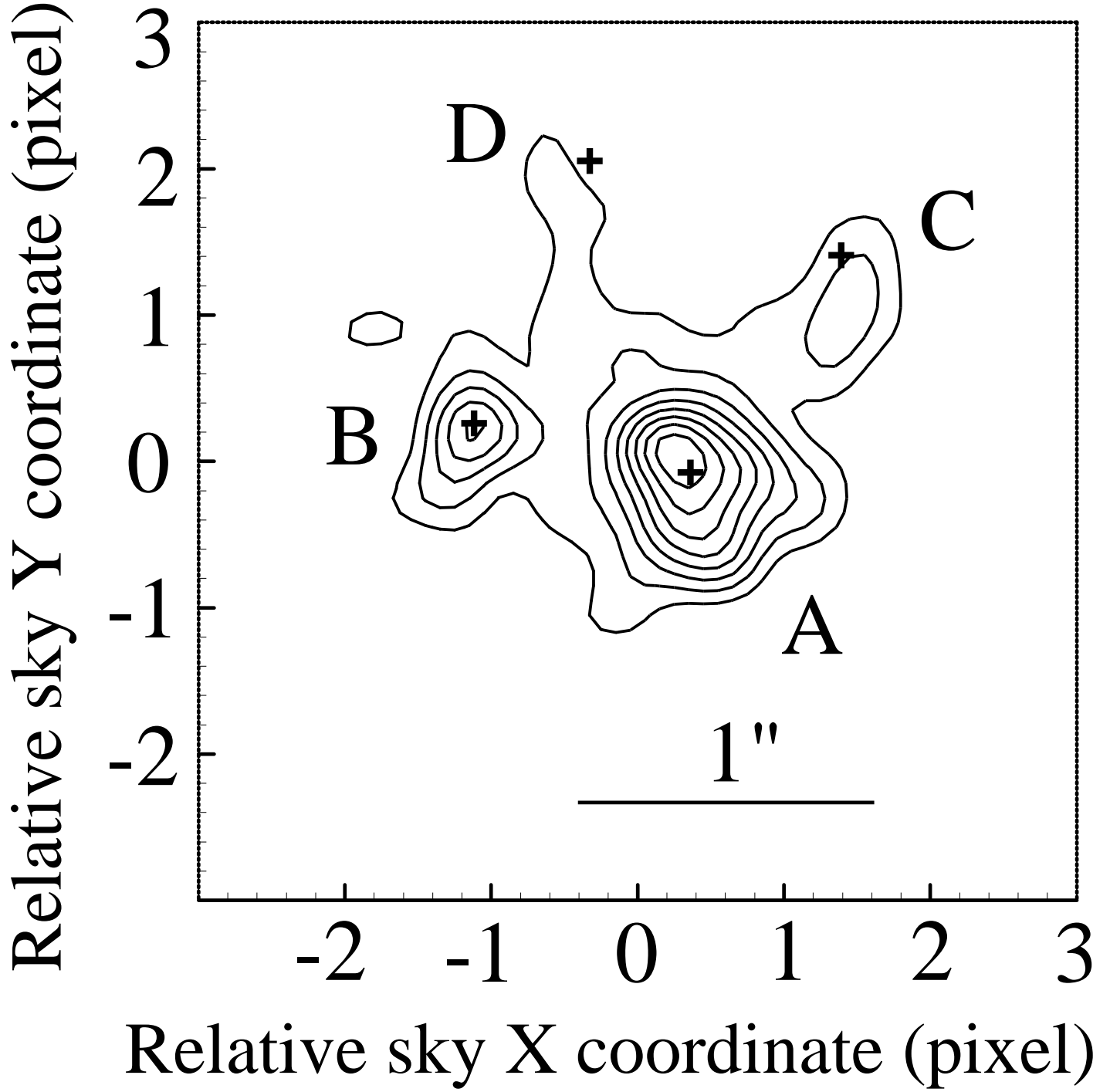


FIG. 1.— ACIS-S image of H1413+117. Shifting the sky coordinates of charge-split events according to the method proposed by Tsunemi et al. (2001), we obtained subpixel spatial resolution. The image is then smoothed with a Gaussian function with a  $\sigma$  of 0.2 pixel size. The X-ray surface brightness is shown with a lowest contour level and an interval of respectively 17 and 8.5 counts/pixel. The image consists of at least three point-like sources. The relative positions of the three sources are consistent with the multiply-lensed images of the QSO A, B, and C at optical wavelengths, which are shown with crosses for reference (Chae & Turnshek 1999). We find a hint of X-ray emission near the the optical position of image D.

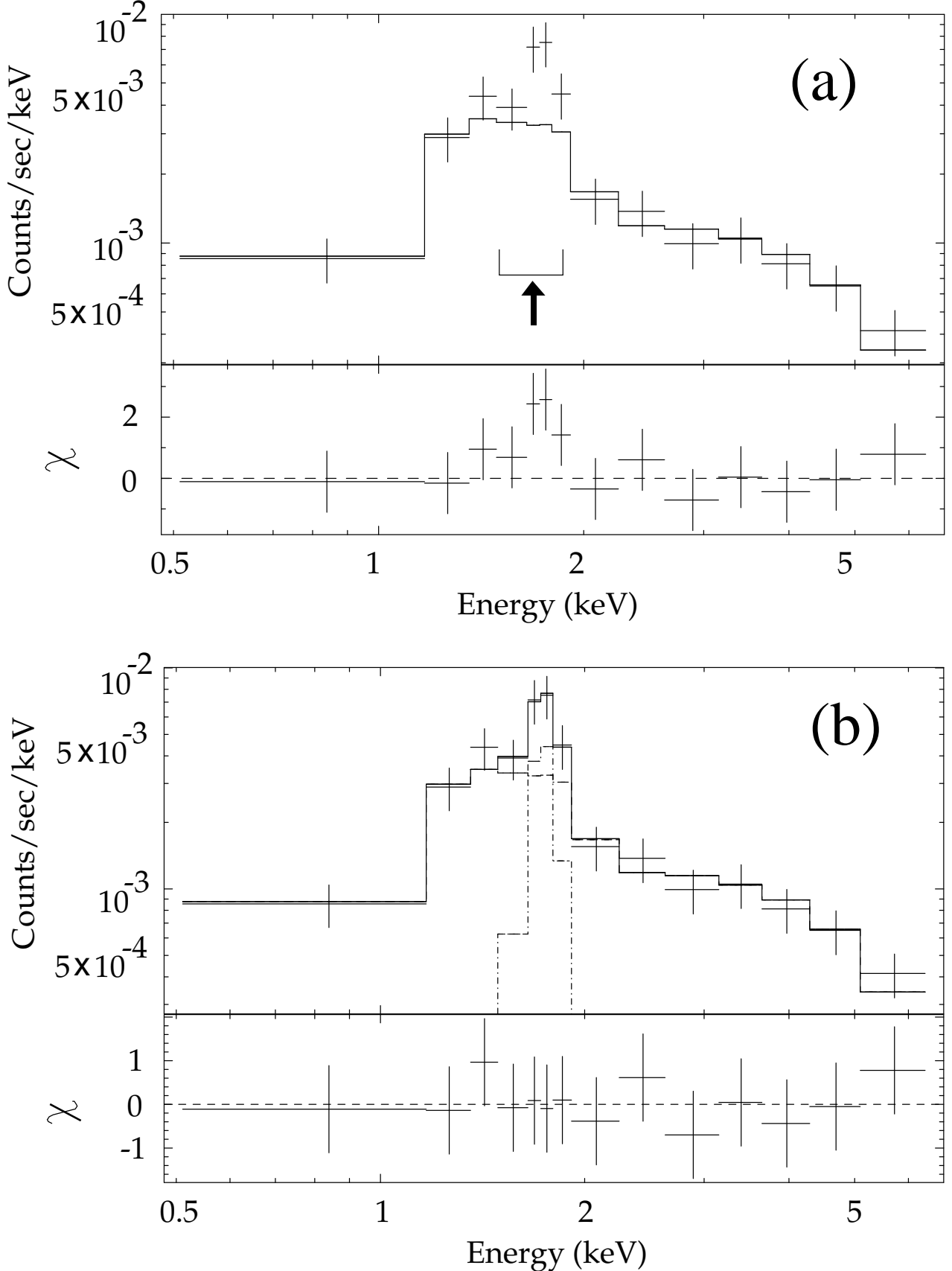


FIG. 2.— Spectral fittings of H1413+117. The observed energy spectrum is shown with crosses and the model functions convolved with the telescope and detector response functions are shown with step functions. (a) An absorbed power-law model was assumed, where the four energy bins marked with an arrow were not used. (b) A Gaussian model was added to the absorbed power-law model, using all the bins. The residual of the fits are shown in the bottom panels. The vertical error bars are  $1-\sigma$  statistical errors.

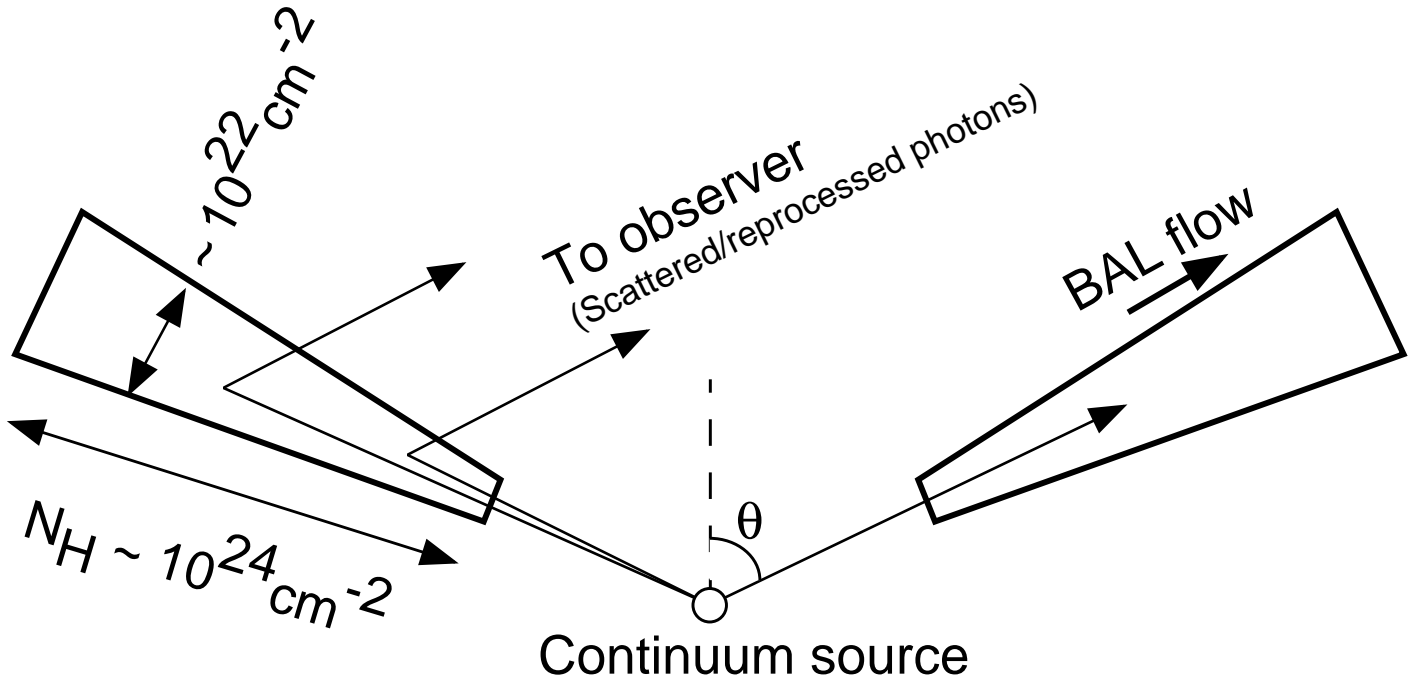


FIG. 3.— Schematic view of the conical BAL-flow model according to the model of Elvis (2000). In this model, the flow is optically thick for the X-ray photons from the central source, but is optically thin for the scattered and the re-emitted photons.